Mobility of Charge Carriers in Sublimed Films of Phenothiazine Derivatives

Sadamu YOSHIDA, Kozo KOZAWA, Yusei MARUYAMA,† and Tokiko UCHIDA*
Department of Industrial and Engineering Chemistry, Faculty of Science and Technology, Science University of Tokyo, Noda, Chiba 278
†Institute for Molecular Science, Myodaiji, Okazaki 444

(Received April 14, 1993)

Mobilities of charge carriers in sublimed films of three phenothiazine derivatives, benzo[*b*]phenothiazine, dibenzo[*a,j*]phenothiazine, and triphenodithiazine, were measured in surface-type cells at room temperature in both transient and stationary phtoconduction. The drift mobilities in films of these three materials, which are the sum of electron and hole mobilities, are on the order of 10^{-7}—10^{-5} cm^2 V^{-1} s^{-1}. They do not seem to be affected by the orientation of molecules in the sublimed films.

We have suggested that the sublimed films of some phenothiazine (PT) derivatives acted as carrier photogeneration layers in photocells, and their conversion efficiency was found to be 10^{-6}—10^{-7}%.[1] A similar order of low conversion efficiency was obtained in other organic photovoltaic cells, and they have been attributed to the low mobilities of carriers.[2—4] So, we attempted to measure carrier mobilities in PT derivative films, to investigate the conduction mechanism of charge carriers in organic sublimed films.

Charge carrier mobilities in organic compounds are usually inferred from time-of-flight experiments for single crystals.[5] However, it is difficult to apply this method to films consisting of assemblies of microcrystals, since the numerous traps in them make an appearance of a typical time-of-flight rectangular curve of the photocurrent impossible. In this paper, we report the carrier mobilities in films of PT derivatives measured by the Maruyama-Baessler method, in which the mobility, μ is estimated by the product of (γ/μ) and (μ^2/γ).[6] The former is assumed from the decay of the transient photocurrent generated by a light pulse, and the latter from the relationship between the stationary photocurrent and the light intensity.

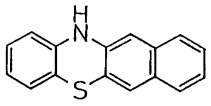

Benzo[b]phenothiazine
(B[b]PT)

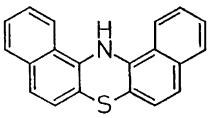

Dibenzo[a,j]phenothiazine
(DB[a,j]PT)

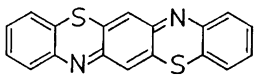

Triphenodithiazine
(TPDT)

Scheme 1. Molecular structures and abbreviations of PT derivatives.

Experimental

Materials and Sample Preparation. Three PT derivatives, benzo[*b*]phenothiazine (B[*b*]PT), dibenzo[*a,j*]-phenothiazine (DB[*a,j*]PT), and triphenodithiazine (TPDT) were synthesized as described in the literature,[7—9] and purified by sublimation in vacuo (Scheme 1). Films of PT derivatives were prepared by vapor deposition at a pressure of 10^{-5} Torr# onto a glass substrate. Absorption spectra of the films were measured by a Hitachi 330 spectrometer, and their thicknesses were measured by a Sloan Dektak 3030 surface profilometer. To prepare blocking electrodes, phenol resin was painted on the films as insulator, then Au paste was painted on top of the structure. A cell assembly is shown in Fig. 1.

Measurements. All the measurements were done in the air at room temperature. Photocurrent pulses, excited by a 1 ns N_2-laser (PRA LN1000) flash, were recorded with an oscilloscope (Tektronix 7834) across a 50 Ω load resistor. Fabrication of cells that were used for transient photocurrent measurements and absorption coefficient of films are shown in Table 1. Stationary photocurrents were excited with 400 nm light, which was filtered by a monochromator (JASCO CT-10), from a 500 W xenon lamp (Ushio UXL-500D) and recorded as a function of light intensity. Fabrication of cells that were used for stationary photocurrent measurements and absorption coefficient of films are shown in Table 2.

Treatment of photocurrent data was done as described in the literature.[6]

1 Torr=133.322 Pa.

Results and Discussion

Transient Photocurrent. Oscilloscope traces of transient photocurrents are shown in Fig. 2. If electron-hole recombination is the dominant mechanism for carrier loss after pulse excitation of a photoconductor, the time decay of photocurrent, $i(t)$ must follow,

$$[i(t)]^{-1} = i_0^{-1} + t/i_0\tau_r, \quad (1)$$

Table 1. Cell Fabrication and Absorption Coefficients of Films of Measurements for Transient Photocurrent

Compound	Length of electrode	Electrode gap	Film thickness	Absorption coefficient for 337 nm light
	l/cm	L/cm	d/cm	α_1/cm^{-1}
B[*b*]PT	0.28	0.05	7.9×10^{-5}	1.8×10^{4}
DB[*a*,*j*]PT	0.32	0.04	7.4×10^{-5}	3.2×10^{4}
TPDT	0.25	0.03	5.0×10^{-5}	2.6×10^{4}

Table 2. Cell Fabrication and Absorption Coefficients of Films of Measurements for Stationary Photocurrent

Compound	Length of electrode	Electrode gap	Film thickness	Absorption coefficient for 400 nm light
	l/cm	L/cm	d/cm	α_2/cm^{-1}
B[*b*]PT	0.20	0.05	1.0×10^{-4}	1.5×10^{4}
DB[*a*,*j*]PT	0.13	0.03	4.2×10^{-5}	2.6×10^{4}
TPDT	0.20	0.05	7.0×10^{-6}	1.5×10^{4}

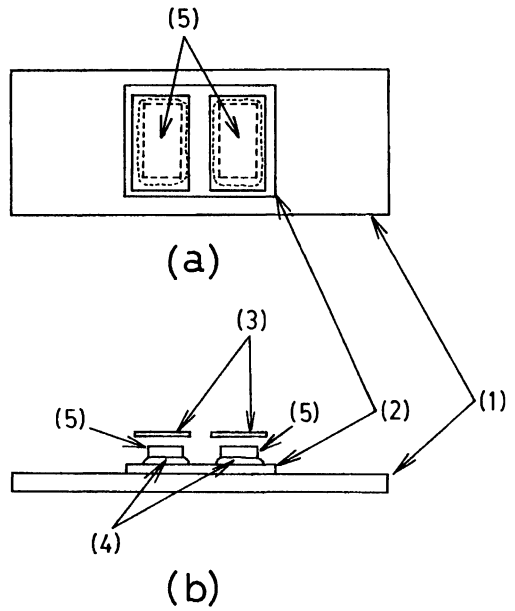

Fig. 1. Cell assembly. (a) Top view, (b) Side view. (1) Pyrex glass; (2) Organic film; (3) Shield; (4) Phenol resin; (5) Electrode.

where i_0 is the initial photocurrent, and τ_r is the recombination time given by $\tau_r=(\gamma n_0)^{-1}\ln 10$ (γ: recombination coefficient, n_0: initial carrier density). Then, $i_0\tau_r$ can be obtained from the slope of the linear relationship between $[i(t)]^{-1}$ and t. The relationships between the reciprocals of $i(t)$ and t for films are shown in Fig. 3, which are point-wise analyses of the oscilloscope trace from Fig. 2. The linear relationships between $[i(t)]^{-1}$ and t were regarded to be fulfilled within the time intervals $50<t<150$ ns for B[*b*]PT film, and $50<t<125$ ns for DB[*a*,*j*]PT and TPDT films. The $i_0\tau_r$ value of each film was obtained by applying Eq. 1.

The ratio of carrier recombination coefficient (γ) and sum of electron and hole mobilities (μ) is given by a function of the experimentally accessible quantity $i_0\tau_r$ as follows,

$$\gamma/\mu = e\alpha_1^{-1}lE\ln 10/i_0\tau_r, \tag{2}$$

where e is the elementary charge, α_1 the absorption coefficient for 337 nm light, l the length of the electrodes, and E the applied electric field. These obtained γ/μ values are shown in Table 3 together with $i_0\tau_r$'s.

Stationary Photocurrent. Under low-light intensity conditions, the stationary photocurrent, i_m, is deduced as follows:

$$i_m = e\psi IlL[1-\exp(-\alpha_2 d)], \tag{3}$$

where ψ is the quantum efficiency for carrier generation, I the incident quantum flux, L the electrode gap, d the sample thickness, and α_2 the absorption coefficient for 400 nm light. At the high-intensity limit, the current, i_b, is represented as,

$$i_b = 2el\mu E\left(\frac{\psi I}{\alpha_2\gamma}\right)^{\frac{1}{2}}\cdot[1-\exp(-\alpha_2 d/2)]. \tag{4}$$

Upon increasing the light intensity the stationary photocurrent should pass from a $I^{1.0}$ to a $I^{0.5}$ law. The extrapolated linear and square root regimes should intersect at an intensity I_{mb}, where $i_m(I_{mb})=i_b(I_{mb})=i_i$. Applying Eqs. 3 and 4 finally yields

$$\frac{\mu^2}{\gamma} = \frac{i_i\alpha_2 L}{4elE^2}\cdot\frac{[1-\exp(-\alpha_2 d)]}{[1-\exp(-\alpha_2 d/2)]^2}. \tag{5}$$

Table 3. Applied Electric Fields and Results of Transient Photocurrents

Compound	E/ V cm^{-1}	$i_0\tau_r$/C	γ/μ/ V cm
B[*b*]PT	6×10^{3}	9.7×10^{-11}	4×10^{-10}
DB[*a*,*j*]PT	1×10^{4}	9.2×10^{-11}	4×10^{-10}
TPDT	2×10^{4}	5.0×10^{-11}	1×10^{-9}

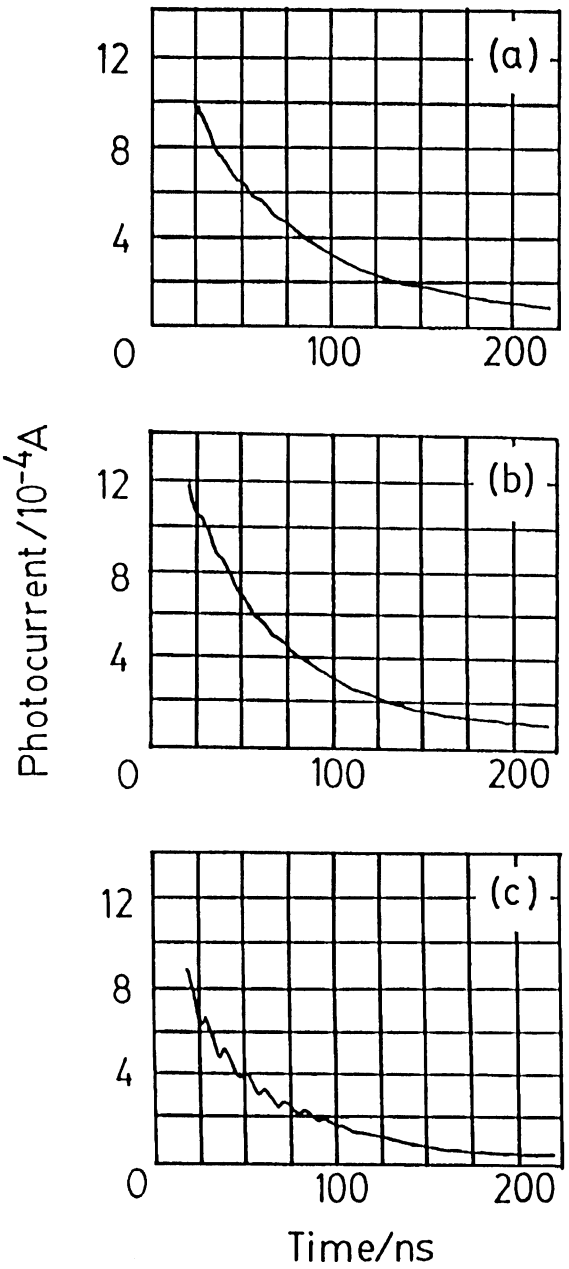

Fig. 2. Oscilloscope traces of photocurrent transients. (a) B[*b*]PT, (b) DB[*a,j*]PT, (c) TPDT.

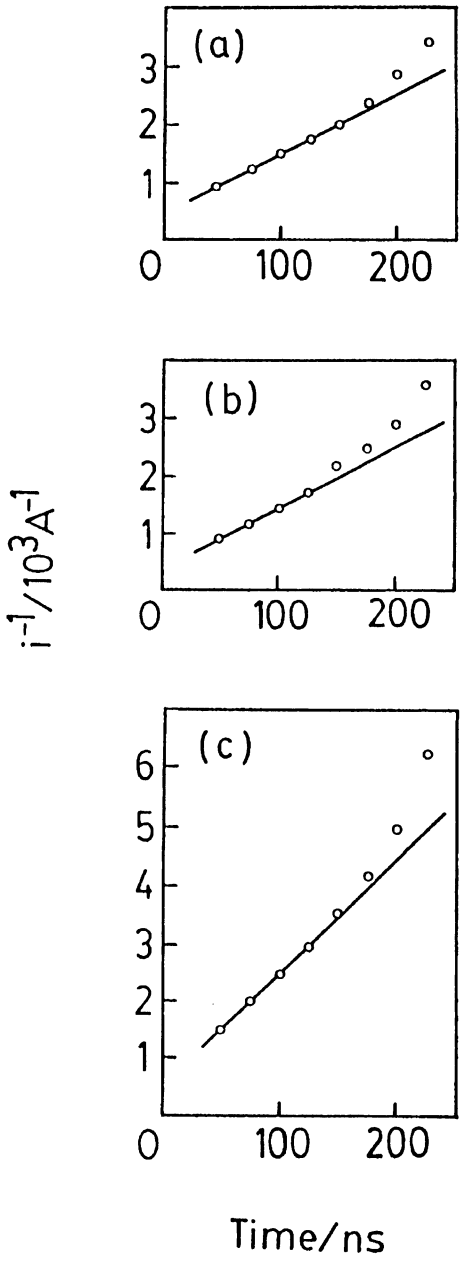

Fig. 3. Point-wise analyses of the oscilloscope traces. (a) B[*b*]PT, (b) DB[*a,j*]PT, (c) TPDT.

Figure 4 illustrates the stationary photocurrent versus light intensity measured for films of three PT derivatives. Experimental data for B[*b*]PT and TPDT films were well in accord with the kinetic model. On the other hand, in the case of DB[*a,j*]PT, the light intensity dependence of photocurrent was proportional to $I^{1.48}$ at the limit of low intensity. So it is possible that photocurrent is generated by another mechanism in this case. Yielding μ^2/γ, E, and i_i of films are shown in Table 4.

Mobilities. Mobilities in films are obtained from the product of γ/μ and μ^2/γ. Yielding mobilities in B[*b*]PT, DB[*a,j*]PT, and TPDT films were 4×10^{-6}, 2×10^{-7}, and 2×10^{-5} cm^2 V^{-1} s^{-1}, respectively. The generally known values of drift mobilities in molecular crystals are on the order of 10^{-2}—1 cm^2 V^{-1} s^{-1}.[10—12] In this experiment, however, mobilities obtained in films are 10^{-7}—10^{-5} cm^2 V^{-1} s^{-1}, somewhat smaller than those in crystals of other organic materi-

Table 4. Applied Electric Fields and Results of Stationary Photocurrents

Compound	E/ V cm^{-1}	i_i/A	μ^2/γ/ cm V^{-2} s^{-1}
B[*b*]PT	4×10^3	1.3×10^{-11}	1×10^4
DB[*a,j*]PT	3×10^3	9.0×10^{-14}	4×10^2
TPDT	6×10^3	3.4×10^{-12}	2×10^4

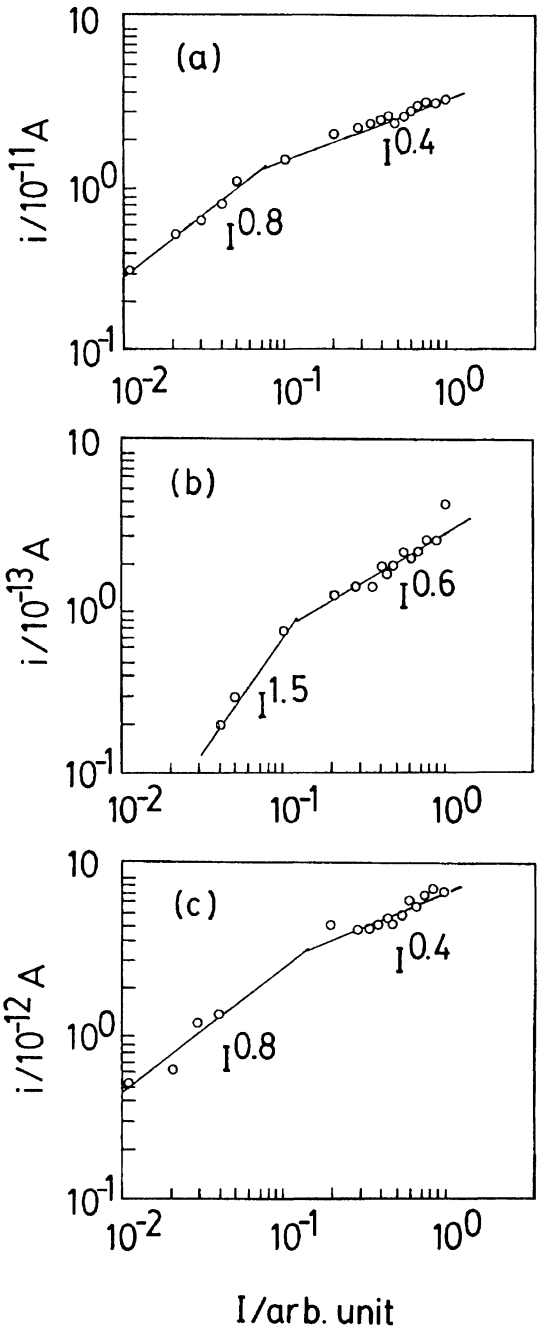

Fig. 4. Stationary photocurrents versus light intensity. (a) B[*b*]PT, (b) DB[*a,j*]PT, (c) TPDT.

als. For these small mobilities, a hopping mechanism may be attributed to the transfer of charge carriers in these films. These small mobilities may be responsible for the low conversion efficiency and low fill factor of the Schottky type cells in which B[*b*]PT, DB[*a,j*]PT, and TPDT are used as photogeneration layers.[1)]

The X-ray diffraction pattern suggests that the molecules stand perpendicularly to the glass substrate only in B[*b*]PT films.[13)] Since the direction of the mobility measurement is parallel to the film plane, this seems to be advantageous for carrier migration. In the direction perpendicular to the film, however, overlaps of molecular planes are quite small, and the mobility of this direction may be smaller than the value observed in B[*b*]PT.

Films of DB[*a,j*]PT, and TPDT did not give any X-ray diffraction peaks.[14)] In any case, it can not be decided from these observations if the molecular arrangement greatly affects the value of carrier mobility in organic films.

The electrical resistivity, ρ, of a pressed powdered sample of TPDT is reported as about 10^{13} Ω cm.[15)] If the resistivity of a TPDT film is assumed to be equal to that of powdered sample, and Eq. 6 can be applied, the carrier density in TPDT film is evaluated as 10^{10} cm^{-3}. Equation 6 is represented as follows,

$$\sigma = ne\mu, \tag{6}$$

where σ is the electric conductivity ($=\rho^{-1}$), n is the carrier density, e is the elementary electric charge, and μ is the mobility. For metal-free phthalocyanine, the carrier density of 10^6 cm^{-3} can be estimated by using the resistivity ($5\times10^{12}\Omega$ cm) and mobility (0.4 cm^2 V^{-1} s^{-1}) values of a single crystal.[16,17)] The carrier density of TPDT film, assumed above, is much greater than that of phthalocyanine, the derivatives of which have been extensively investigated as organic photocarrier generation layers.[18—20)] Therefore, TPDT film is expected to function as a good photogeneration layer.

References

1) S. Yoshida, K. Kozawa, and T. Uchida, "Symposium on Molecular Structure," Fukuoka, October 1990, Abstr., No. 2aP36.
2) M. Yokoyama, *Kobunshi*, **34**, 728 (1985).
3) Y. Shirota, *Kobunshi*, **38**, 346 (1989).
4) Y. Shirota, *Kagaku Kogyo*, **35**, 790 (1984).
5) R. G. Kepler, *Physical Review*, **119**, 1226 (1960).
6) Y. Maruyama and H. Baessler, *Phys. Status Solidi B*, **103**, 263 (1981).
7) J. A. van Allan, G. A. Reynolds, and R. E. Ader, *J. Org. Chem.*, **27**, 1659 (1962).
8) F. Kahrmann, *Ann.*, **322**, 51 (1902).
9) J. Garbarczyk and A. Zuk, *Phosphorus Sulfur*, **6**, 351 (1979).
10) J. H. Sharp, *J. Phys. Chem.*, **71**, 2587 (1967).
11) H. Kitayama, M. Yokoyama, and H. Mikawa, *Mol. Cryst. Liq. Cryst.*, **69**, 257 (1981).
12) H. Kitayama, M. Yokoyama, and H. Mikawa, *Mol. Crystl. Liq. Cryst.*, **76**, 19 (1981).
13) Crystal data of B[*b*]PT are as follows: monoclinic, $P2_1/n$, $a=25.856(6)$, $b=7.838(2)$, $c=5.856(1)$ Å, $\beta=95.02(2)°$, $V=1183.7(7)$ Å^3, $Z=4$. X-ray crystal structure analysis is not complete because of a structural disorder (present $R=0.155$). The observed diffraction peaks of a B[*b*]PT film correspond to (*h*00) planes, which means that B[*b*]PT molecules stand perpendicularly to the substrate according to our preliminary structural analysis.
14) On the observation with polarizing microscope, a

complete dark image was not given for DB[*a,j*]PT and TPDT films with crossed Nicols. So these films are not considered to be amorphous but microcrystalline.

15) I. Shirotani, N. Sato, H. Nishi, K. Fukuhara, T. Kajiwara, and H. Inokuchi, *Nippon Kagaku Kaishi*, **1986**, 485.

16) G. H. Heilmeier and G. Warfield, *J. Chem. Phys.*, **38**, 163 (1963).

17) F. Gutmann and L. E. Lyons, "Organic Semiconductors," John Wiley & Sons, New York (1967), p. 714.

18) F. R. Fan and L. R. Faulkner, *J. Chem. Phys.*, **69**, 3341 (1978).

19) T. Tanaka and R. Hirohashi, *Nippon Kagaku Kaishi*, **1989**, 867.

20) T. Morikawa, C. Adachi, T. Tsutsui, and S. Saito, *Nippon Kagaku Kaishi*, **1990**, 962.